

---

---

# COMPUTER-SIMULATION SURROGATES FOR OPTIMIZATION: APPLICATION TO TRAPEZOIDAL DUCTS AND AXISYMMETRIC BODIES

John C. Otto

Department of Aeronautics and Astronautics, M.I.T.  
Multidisciplinary Design Optimization Branch  
NASA Langley Research Center  
Hampton, Virginia

Marius Paraschivoiu, Serhat Yeşilyurt, and Anthony T. Patera

Department of Mechanical Engineering  
Massachusetts Institute of Technology  
Cambridge, Massachusetts

## ABSTRACT

Engineering design and optimization efforts using computational systems rapidly become resource intensive. The goal of the surrogate-based approach is to perform a complete optimization with limited resources. In this paper we present a Bayesian-validated approach that informs the designer as to how well the surrogate performs; in particular, our surrogate framework provides precise (albeit probabilistic) bounds on the errors incurred in the surrogate-for-simulation substitution. The theory and algorithms of our computer-simulation surrogate framework are first described. The utility of the framework is then demonstrated through two illustrative examples: maximization of the flowrate of fully developed flow in trapezoidal ducts; and design of an axisymmetric body that achieves a target Stokes drag.

## INTRODUCTION

Computational design efforts typically consist of a sequence of optimization problems characterized by different combinations of design parameters and objective functions. Each design problem is solved by means of a nonlinear optimization algorithm. Numerical simulations can be incorporated into the optimization algorithm either by *direct-insertion* or through a *surrogate-based* approach. In *direct-insertion*, the large-scale simulation is inserted into the optimization algorithm as a function call. In the *surrogate-based* approach, a surrogate (a simple model such as a response surface) for the simulation is first constructed, and the surrogate is then incorporated into the optimization algorithm in place of the full simulation.

Many optimization problems based upon *direct-insertion* are hindered, first, by the cost of each inquiry to the simulation code, and second, by the algorithmic difficulties of merging the large-scale simulation with the mathematical programming algorithm. Furthermore, the high cost of objective-function evaluations for the direct-insertion method reduces the interactivity of the design process. Finally, the number of objective-function evaluations required to achieve the optimal solution is typically not known *a priori*, and computational resources may thus be exhausted before a feasible design is achieved. The latter is especially pronounced in the case of multidisciplinary optimization (Newman et al., 1992).

To circumvent these difficulties, we pursue a *surrogate-based* approach to optimization (McKay et al., 1979; Sacks et al., 1989; Barthelemy and Haftka, 1993; and Yeşilyurt and Patera, 1995). The surrogate approach offers a number of advantages. First, by construction, surrogate evaluations require very little computational effort, and are thus easily incorporated into optimization procedures. Second, the very low computational requirement permits a more complete optimization by assuring that computational resources will not be exhausted before the design is complete. Third, surrogates create highly interactive and flexible design environments, allowing multiple optimization tasks characterized by different design parameters to be pursued more easily.

As regards disadvantages, the most important drawback is that surrogate-based optimization introduces a new source of error. A surrogate validation strategy and appropriate error norms must be developed to

quantify the discrepancy between the surrogate and the actual simulation, and to estimate the errors in system *predictability* and *optimality*. The former provides a bound on the behavior of the actual objective function in the neighborhood of the surrogate minimizer, while the latter provides a bounding region in which the actual minimizer lies.

In this paper, we first describe the optimization problem which is central to the remainder of the paper. We then briefly review our baseline surrogate framework, and offer references to more detailed descriptions. Next, we present several improved surrogate algorithms that have been developed. In the final section of the paper, we apply the surrogate framework to two design optimization problems: optimization for pressure–driven flow in a trapezoidal duct; and shape optimization for Stokes flow past an axisymmetric body.

## OPTIMIZATION

The minimizer to the exact optimization problem is given by

$$\mathbf{p}^* = \arg \min_{\mathbf{p} \in \Omega} |\mathcal{S}(\mathbf{p}) - \lambda|, \quad (1)$$

where  $\mathbf{p}$  is the vector of  $M$  design inputs which lie in the input (or “design”) domain  $\Omega \subset \mathbb{R}^M$ ,  $\mathcal{S}(\mathbf{p})$  is the input–output relation, and  $\lambda$  is the target value. This problem is also referred to as a “discrimination” problem (Seber and Wild, 1989). More general objective functions are examined in Yesilyurt (1995), and Yesilyurt and Patera (1995).

As already described, direct insertion of the full simulation for  $\mathcal{S}(\mathbf{p})$  in equation (1) is impractical. Instead, a surrogate,  $\tilde{\mathcal{S}}(\mathbf{p})$ , for the simulation is inserted into the optimization problem. The minimizer for the resulting surrogate–based optimization problem is given by

$$\tilde{\mathbf{p}}^* = \arg \min_{\mathbf{p} \in \Omega} |\tilde{\mathcal{S}}(\mathbf{p}) - \lambda|. \quad (2)$$

The optimization then proceeds as for direct–insertion, but the surrogate is evoked instead of the simulation.

The advantages of using a surrogate framework for optimization have already been described. The issues of *predictability* and *optimality* must be addressed (Bohlin, 1991). For *predictability*, we are concerned with how the actual simulation behaves in the vicinity of the surrogate–predicted minimizer,  $\tilde{\mathbf{p}}^*$ . We seek to be able to bound  $|\tilde{\mathcal{S}}(\mathbf{p} \approx \tilde{\mathbf{p}}^*) - \mathcal{S}(\tilde{\mathbf{p}}^*)|$ , and also to ensure that this bound is acceptably small. The proximity of  $\tilde{\mathbf{p}}^*$  to  $\mathbf{p}^*$ , the actual optimizer, (i.e. *optimality*), is also important, although not as critical in this context as *predictability*. The validation strategy which yields *predictability* statements is addressed next.

## SURROGATE FRAMEWORK

The Bayesian–validated surrogate methodology presented here has the distinguishing attribute of integrating a complete and rigorous validation framework. The outcome of the validation step is fully incorporated into the *a posteriori* purposive analysis, and hence the predictability of any optimization is a natural extension of the validation. The validation itself is based on the results of order statistics (David, 1981) where the validation sample size ( $N^{va}$ ) is determined *a priori*. In this section, we briefly describe the baseline surrogate–validation algorithm and *a posteriori* error analysis framework. A full description, and additional algorithms, can be found in Paraschivoiu (1995) and Otto et al. (1995).

### A Baseline Approach

We first define a model prediction error estimator:

$$U = \max_{\mathbf{p} \in \mathcal{X}_{\mathbf{p}}^{va}} |R_j - \tilde{\mathcal{S}}(\mathbf{p})|, \quad (3)$$

where  $\mathcal{X}_{\mathbf{p}}^{va}$  is a random set of  $N^{va}$  points in  $\Omega$  distributed according to an importance function  $\rho(\mathbf{p})$ . Then, given a vector of “uncertainty” parameters ( $\Theta$ ) we can calculate the required sample size. Two different predictability statements have been developed: “Prediction Region” ( $\mathcal{PR}$ ) and “Proximal–Candidate” ( $\mathcal{PC}$ ). The former gives a predictability statement for a region neighboring the surrogate–based optimum,  $\tilde{\mathbf{p}}^*$ , while the latter evaluates the predictability of a specific nearby candidate design.

The validation sample sizes for each approach are

$$\mathcal{PR} : \quad N^{va} \equiv \ln \varepsilon_2 / \ln(1 - \varepsilon_1), \quad (4)$$

$$\mathcal{PC} : \quad \varepsilon_2 = \frac{1}{\eta(N^{va} + 1)} \left( 1 - (1 - \eta)^{N^{va} + 1} \right), \quad (5)$$

where  $\Theta = (\varepsilon_1, \varepsilon_2) \in (0, 1)^2$  in equation (4) and  $\Theta = (\eta, \varepsilon_2) \in (0, 1)^2$  in equation (5).

### A Posteriori Error Analysis

Two approaches to the error analysis of our surrogate–predicted optimum points are presented. The first is a “Prediction Region” approach and the second is a “Proximal–Candidate” based approach. Both of these analyses seek to address the *predictability* concerns already described.

**Prediction Region.** The inputs to the “Prediction Region” error analysis are the model prediction error,  $U$ , from the surrogate validation, and the surrogate–predicted optimizer  $\tilde{\mathbf{p}}^*$ . We introduce a parameter,  $\eta$ ,

$\varepsilon_1 < \eta < 1$ , and construct a region,  $\mathcal{R}$  such that

$$\int_{\mathcal{R}} \rho(\mathbf{p}) d\mathbf{p} = \eta. \quad (6)$$

Here,  $\mathcal{R}$  is typically chosen as that region,  $\mathcal{R}'$ , of  $\rho$ -measure  $\eta$  which minimizes  $\Delta_{max}$ , the maximum distance,  $\Delta(\mathbf{p}', \tilde{\mathbf{p}}^*)$ , between all points  $\mathbf{p}' \in \mathcal{R}'$  and  $\tilde{\mathbf{p}}^*$ . The distance  $\Delta(\cdot, \cdot)$  can be any valid distance between  $\mathbf{p}'$  and  $\tilde{\mathbf{p}}^*$ .

Introducing a surrogate sensitivity parameter

$$\delta = \max_{\mathbf{p} \in \mathcal{R}} |\tilde{\mathcal{S}}(\mathbf{p}) - \tilde{\mathcal{S}}(\tilde{\mathbf{p}}^*)|, \quad (7)$$

the following statement can be made: There exists many points,  $\hat{\mathbf{p}}$ , in the region  $\mathcal{R}$  such that, with probability greater than  $1 - \varepsilon_2$ ,

$$|\mathcal{S}(\hat{\mathbf{p}}) - \lambda| \leq |\tilde{\mathcal{S}}(\tilde{\mathbf{p}}^*) - \lambda| + \varpi, \quad (8)$$

where  $\varpi = U + \delta$  is the *predictability*-gap. This statement provides a probabilistic bound on the actual system performance,  $|\mathcal{S}(\hat{\mathbf{p}}) - \lambda|$ , for points,  $\hat{\mathbf{p}}$ , near the surrogate-predicted optimum,  $\tilde{\mathbf{p}}^*$ . Recall that the number of simulations to obtain  $U$  is given by Equation (4).

**Proximal-Candidate.** In many problems it may be difficult, or even impossible, to explicitly construct prediction regions  $\mathcal{R} \subset \Omega$  as described in the last section. Another approach is to only *observe* the prediction region (and not *construct* the region) through sample candidate designs,  $\hat{\mathbf{P}}^*$ , which, with a prescribed probability, will exhibit actual performance within the predictability gap of the surrogate-predicted optimal performance. We refer to this method as a “Proximal-Candidate” approach to *a posteriori* analysis (Otto, 1995, and Otto et al., 1995).

The two inputs to the validation are  $\eta$  and  $\varepsilon_2$ , where  $0 < \eta, \varepsilon_2 < 1$ . In the *a posteriori* analysis, we introduce that region  $\mathcal{R} \subset \Omega$  which satisfies Equation (6) and minimizes  $\Delta_{max}$ , and sample a  $\hat{\mathbf{P}}^* \in \mathcal{R}$  according to the probability density

$$\rho_{\mathcal{R}}(\mathbf{p}) = \frac{1}{\eta} \rho(\mathbf{p})|_{\mathcal{R}} \quad \forall \mathbf{p} \in \mathcal{R}. \quad (9)$$

Using acceptance-rejection techniques, the region  $\mathcal{R}$  can be measured and sampled without actually constructing the region.

The *a posteriori* error statement (similar to the “Prediction Region” result) is

$$\Pr\{|\mathcal{S}(\hat{\mathbf{P}}^*) - \lambda| \leq |\tilde{\mathcal{S}}(\tilde{\mathbf{p}}^*) - \lambda| + \varpi'\} \geq 1 - \varepsilon_2, \quad (10)$$

where  $\varpi' = U + \delta'$  is the predictability gap and  $\delta' = |\tilde{\mathcal{S}}(\hat{\mathbf{P}}) - \tilde{\mathcal{S}}(\tilde{\mathbf{p}}^*)|$ . In words, Equation (10) says that, with

probability greater than  $1 - \varepsilon_2$ , there will exist a candidate design  $\hat{\mathbf{P}}^*$  for which actual system performance,  $|\mathcal{S}(\hat{\mathbf{P}}^*) - \lambda|$ , is within  $\varpi'$  of the surrogate-predicted optimum objective value,  $|\tilde{\mathcal{S}}(\tilde{\mathbf{p}}^*) - \lambda|$ . The number of validation points needed is given by Equation (5).

Finally, we remark that the “uncertainty” vector  $\Theta$  measures the degree of precision with which the surrogate must be validated. As  $\varepsilon_1$ ,  $\varepsilon_2$ , and  $\eta$  decrease, the number of validation points increases, and more information as to the quality of the surrogate is extracted. The probabilistic framework results in a fixed validation sample size, allowing the designer to tune the “uncertainty” vector to the available resources.

## IMPROVED ALGORITHMS

In this section we describe several improvements to the baseline algorithm that have been developed. A full description of the additional algorithms can be found in Paraschivoiu (1995).

### Elemental Algorithm

One of the shortcomings of the baseline approach to validation is the global nature of the model prediction error  $U$ . That is, a large error at one point of the input space has a dominating influence over the entire input space. One way to address this drawback is to divide the input domain,  $\Omega$ , into  $L$  non-overlapping, elements (or sub-domains) (Paraschivoiu, 1995; Otto et al., 1995). Validation is performed independently on each sub-domain yielding a local model prediction error,  $(U^\ell, \ell = 1, \dots, L)$ , associated with each element,  $\Omega^\ell$ . The  $U^\ell$  for each element is then used in the *a posteriori* error analysis.

For the elemental algorithm, the size of the validation sample for each element,  $N^{va\ell}$ , is

$$\mathcal{PR} : \quad N^{va\ell} \equiv \frac{\ln(1 - (1 - \varepsilon_2)^{1/L})}{\ln(1 - L\varepsilon_1)}, \quad (11)$$

$$\mathcal{PC} : \quad \varepsilon_2 = 1 - LN^{va\ell}, \quad \int_0^{\eta L} \left(1 - \frac{z}{\eta L}\right) \left(1 - (1 - z)^{N^{va\ell}}\right)^L (1 - z)^{N^{va\ell}-1} dz. \quad (12)$$

The locality improvement in the model prediction error estimator is obtained with a small increase in the number of validation points for small numbers of elements. For a very large number of elements, even *fewer* validation points are needed than for a single element.

## Cross-Validation, Re-Sampling

A natural extension of the elemental algorithm for the  $\mathcal{PR}$  approach is an intra-model, cross-validation procedure (Paraschivoiu, 1995) which allows the use of the available simulation data for both construction and validation. Indeed, due to the elemental partitioning, the validation data from one element can be used for the construction of a surrogate model in another element. The only restriction is an ordered dependence requirement, which means that validation data can only be used for construction in higher numbered elements (with respect to some ordering).

## Model-Sequential Approach

To achieve a desired target level for the model prediction error estimator, a model-sequential approach is pursued. We assume that we are given a sequence of  $J$  models,  $\tilde{\mathcal{S}}_j(\mathbf{p})$ ,  $j = 1, \dots, J$ , and a *desired* model prediction error,  $\alpha > 0$ . The sequential algorithm validates each subsequent model with the same points as used for the previous model plus one new random validation point. If, for the  $j^{th}$  model, the model prediction error estimator is less than or equal to  $\alpha$ , then that model is selected. If, on the other hand, all the models have been tested, and none has satisfied the *desired* model prediction error, then the last model is selected. Respectively,  $\alpha$  or  $U^J$  then serves as the model prediction error estimator in the *a posteriori* analysis. The initial number of validation points is given by

$$N^{va(0)} = \ln \left( \frac{\varepsilon_1 \varepsilon_2}{1 - (1 - \varepsilon_1)^J} \right) / \ln(1 - \varepsilon_1) - 1. \quad (13)$$

## An Adaptive, Model-Sequential Approach

To integrate construction into the model-sequential approach, an adaptive algorithm is considered. In this algorithm, simulation evaluations used for the validation of previous models are incorporated into the surrogate construction, and a new set of validation points is chosen for each subsequent validation. The size of each sample set (assuming  $J$  finite) is

$$N^{va} = \ln \left( \frac{\varepsilon_2}{J} \right) / \ln(1 - \varepsilon_1). \quad (14)$$

The desired model prediction error,  $\alpha$ , is used as previously described in the model-sequential approach. In practice, this approach is very powerful for the construction of surrogates that achieve the desired model prediction error. However, the cost of evaluating a new set of validation points at each step is expensive. This drawback is currently under investigation.

We conclude by commenting that the elemental partitioning can be incorporated in both the sequential and the adaptive methods. This combination offers significant advantages in obtaining the desired local model prediction error with a minimal number of validation points. Indeed, in some elements, the desired elemental model prediction error can be reached faster than in others, and the iterative process stopped in those elements.

## APPLICATIONS

### Flow in a Trapezoidal Duct

As our first illustrative example, we consider fully developed laminar fluid flow in a duct of constant trapezoidal cross-section. The optimization problem is to determine the geometry, for a given cross-sectional area  $A_0$ , that achieves a target flowrate. In this problem the pressure gradient is fixed. The trapezoidal geometry is defined by two inputs; the angle between the base and the side, and the height normalized with respect to the base length. The non-dimensional form  $(\hat{\cdot})$  of the Poiseuille flow equation inside the duct  $(\mathcal{D})$ , with non-slip boundary conditions on the walls  $(\mathcal{B})$  is

$$\begin{cases} \nabla^2 \hat{u} = -1 & \text{in } \mathcal{D} \\ \hat{u} = 0 & \text{on } \mathcal{B} \end{cases}. \quad (15)$$

Using non-dimensional variables we relate the normalized flowrate to the geometrical properties. We first write the pressure drop  $(\Delta P)$  as a function of the friction factor. Knowing that, for laminar flow, the friction factor is simply a shape-dependent constant  $g$  over the Reynolds number, we can obtain an expression for the dimensional flowrate; here the Reynolds number is taken with respect to the hydraulic diameter of the dimensionless trapezoidal section,  $\hat{D}_h$ . The normalized flowrate can be written

$$\hat{Q} = \frac{Q}{\frac{2\Delta P}{\mu L} A_0^2} = \frac{\hat{D}_h^2}{g \hat{A}} = \frac{\bar{\hat{u}}}{2 \hat{A}}, \quad (16)$$

where  $L$  is the length of the duct,  $\mu$  is the dynamic viscosity of the fluid, and  $\bar{\hat{u}}$  is the non-dimensional cross-sectional average velocity.

Equation (16) is useful in incorporating prior information on particular geometries through different values of  $g$ . In addition, we see that our optimization problem is simplified by the absence of scale dependency, that is, our solution is independent of the cross-sectional area,  $A_0$ , of the dimensional duct. The optimization problem is a simple inverse-simulation type: find the input geometry  $(\hat{h}^*, \theta^*)$  that minimizes the difference between the target  $\lambda$  and the numerical solution

of the normalized flowrate. That is,

$$(\hat{h}^*, \theta^*) = \arg \min_{(\hat{h}, \theta) \in \Omega} |\mathcal{S}(\hat{h}, \theta) - \lambda| \quad (17)$$

where  $\lambda = \frac{Q_{desired}}{\frac{2\Delta P}{\mu L} A_0^2}$ , and  $\mathcal{S}(\hat{h}, \theta) \equiv \frac{\bar{u}}{2\hat{A}}$ .

To obtain the velocity field in the trapezoidal channel, a numerical approximation scheme is used to solve Equation (15). In particular, we employ a second order finite element method on triangular elements in  $\mathbb{R}^2$  with automatic mesh generation and conjugate gradient iterative solution. For all geometries, approximately 4500 degrees-of-freedom are used, and each evaluation of the flowrate takes approximately 10 seconds on a single processor of a HP9000/735 workstation. The numerical results can be considered to have a normalized  $\ell_\infty$  error norm less than  $5 \times 10^{-4}$ , which motivates us to consider these results to be without “noise” (Yeşilyurt et al., 1995).

**Surrogate approach.** The design (or input) space covers different trapezoidal geometries ranging from a rectangle to an isosceles triangle. Small clearance limits are included to yield the following input space:

$$\Omega = \left\{ (\hat{h}, \theta) \mid 0.01 \leq \hat{h} \leq \min(\tan \theta, 4.0); 0.05 \leq \theta \leq \frac{\pi}{2} \right\}. \quad (18)$$

In all cases the importance function is taken to be uniform. We first apply the baseline algorithm to find the trapezoidal geometry that achieves a target normalized flowrate. In this first optimization exercise, we consider only variation of the height of the section, while fixing the angle of the trapezoid to  $\frac{\pi}{2}$ ; the corresponding “slice” of  $\Omega$ ,  $[0, 0, 0.5]$ , is denoted  $\Omega'$ .

The four steps of the surrogate-based optimization are as follows. First, we construct a surrogate based on prior information only; in particular, we take  $g = 53.33$  (the known value for an equilateral triangle) in Equation (16). In Figure 1, the normalized flowrate is plotted versus the dimensionless height, and the surrogate is shown by the solid line. Second, we use this surrogate to find the height ( $\tilde{p}^*$ ) corresponding to the desired target flowrate,  $\lambda = 0.01$ . Third, we wish to know how well our surrogate has performed. To obtain this information, validation is carried out. The number of validation points, that is the number of calculations of the flowrate for random height values, is obtained from Equation (4). For  $\varepsilon_1 = \varepsilon_2 = 0.2$ , eight validation points are needed. These points are represented by circles on Figure 1. The maximum difference between the surrogate and the exact simulation value of the normalized flowrate over all the validation points determines the model prediction error estimator,

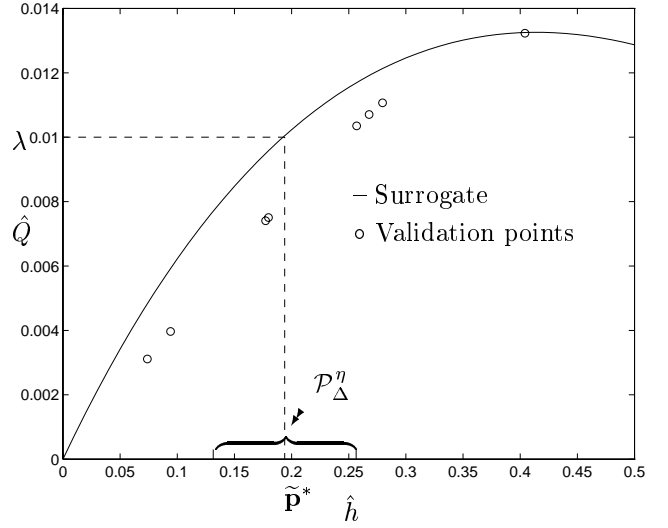


Figure 1: Surrogate for duct flow example using the “baseline” algorithm.

*U*. Fourth, and finally, we can make the following *predictability* statements: With probability  $> 0.8$  ( $1 - \varepsilon_2$ ); **(a)** the surrogate error is less than  $U = 15.8\%$  over at least 80% ( $1 - \varepsilon_1$ ) of the input domain  $\Omega'$ , and, **(b)** there exists many points in the prediction neighborhood of the surrogate optimum geometry  $\tilde{p}^*$ ,  $\mathcal{P}_\Delta^n$ , where the exact simulation is within 34.6% of the target flowrate, normalized by the maximum value of the surrogate.

The *predictability* statement indicates **(a)** quantitatively how good the surrogate is over the entire domain, and **(b)** how well it performs in the neighborhood of the actual optimum. The neighborhood is indicated on the figure by  $\mathcal{P}_\Delta^n$ . This example is useful to demonstrate not how well we can construct a surrogate, but rather, what can be said about the surrogate once it is constructed. In this case, we see that our model does not perform very well.

One way to decrease the error estimate, for a given construction, is to decompose the input space into elements and validate the surrogate in each element. We divide the input space into eight different elements (shown in Figure 2). In addition, we use the cross-validation algorithm to simultaneously construct and validate as follows: First, element one is constructed using prior information (no flow at  $\hat{h} = 0$ ) and only one construction point. Second, this surrogate is validated with three validation points. Third, the points used to validate the surrogate in the current element are used to construct the surrogate in the next element with a quadratic extrapolation. The second and third steps are repeated until surrogates are constructed and validated in all of the elements. This procedure results in a surrogate with a local  $U$  of less than 0.8% in each ele-

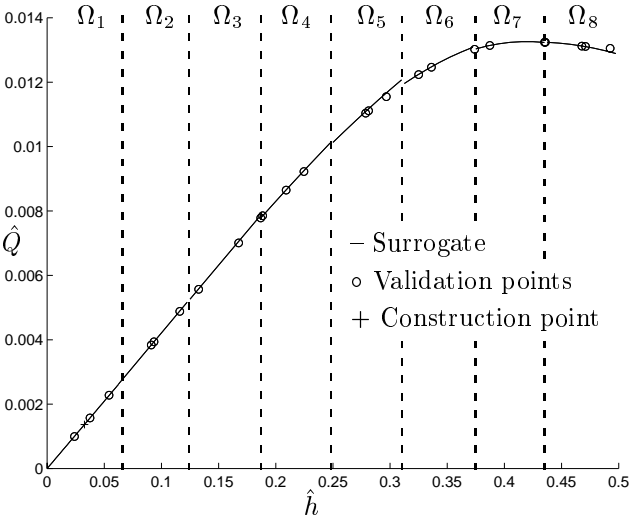


Figure 2: Surrogate for duct flow example using the “Elemental” algorithm.

ment. This surrogate (solid line in Figure 2) can now be used similarly to the baseline algorithm, and surrogate-based optimization can be pursued. The predictability statement is improved due to the use of the local model prediction error.

Finally, the adaptive algorithm is applied to demonstrate the surrogate framework for a two-dimensional input space. The “uncertainty” vector,  $\Theta$ , is set to  $\Theta = (\varepsilon_1, \varepsilon_2) = (0.05, 0.10)$ . We limit ourselves to at most five models ( $J = 5$ ) constructed using Shepard’s algorithm (Shepard, 1968), with which we wish to achieve a model prediction error of less than 5% ( $\alpha = 8.8 \times 10^{-4}$ ). From Equation (14), the number of validation points needed for each validation step is 77. The target error was achieved with the second surrogate and required 127 simulations for construction. The first model had 50 construction points and performed with a 7.8% model prediction error estimate. Therefore, a second surrogate was needed. For this surrogate, the 77 points used to validate the first surrogate were used, along with the original 50 construction points, to achieve the target error.

The surrogate-based maximization of the flowrate yields  $\hat{h}^* = 0.99$ ,  $\hat{\theta}^* = 1.55$ ,  $\tilde{\mathcal{S}}(\hat{h}^*, \hat{\theta}^*) = 1.76 \times 10^{-2}$ . Figure 3 shows isocontours of the normalized flowrate given by the surrogate model, the surrogate-predicted optimum geometry, and the prediction neighborhood. Based on the validation step and the *a posteriori* error analysis, the predictability statements read, with probability  $\geq 0.9$ : (a) the surrogate error is less than  $\alpha = 5\%$  over at least 95% of the input domain  $\Omega(\hat{h}, \theta)$ , and, (b) there exists many points in the prediction neighborhood of the surrogate optimum geometry  $\tilde{\mathbf{p}}^*$ ,

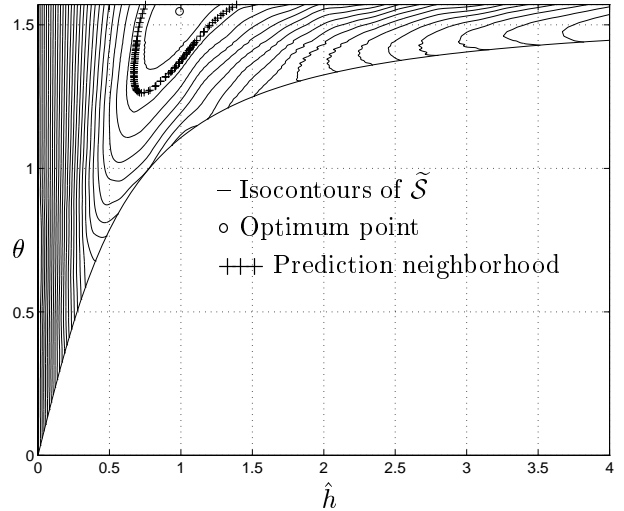


Figure 3: Surrogate for duct flow example using the “adaptive” algorithm.

$\mathcal{P}_\Delta^\eta$ , where the exact simulation is within 8.9% of the target flowrate.

The exact solution to this optimization problem is a square cross-section geometry. We can compare this with our surrogate-based optimization on Figure 3 and observe that they are very close. In addition, the difference between the maximum normalized flowrate predicted by the surrogate and predicted by the simulation is less than 0.1%. This is well within the model prediction error estimate. For this optimization problem, we see that sharp results can be obtained at the expense of increased cost. In practice, this cost could be decreased by using combinations of the previous algorithms.

We conclude by acknowledging that this test case falls short of completely illustrating the advantages of the surrogate framework. For example, due to the relatively inexpensive computations, and because the objective function is smooth, a direct insertion approach could be used. However, for multiple design optimizations, direct insertion, even in this case, can be prohibitively expensive compared to the surrogate framework. Furthermore, in practice, most engineering optimization studies require expensive simulations (Yeşilyurt et al., 1995; Yeşilyurt and Patera, 1995).

### Shape Optimization

Many engineering design problems involve not only *configuration* optimization, in which optimal values of a small number of parameters (e.g. radius, position, angle, etc.) are desired, but also *shape* optimization, in which the optimal form of a curve is desired. Given the deterioration of volume-based error estimates present for problems with high input dimensions, it would ap-

pear that shape optimization problems (described exactly by an *infinite*-dimensional input space) would be intractable in this framework. This is not the case, however, primarily due to two reasons. First, highly irregular shapes will typically be non-optimal, allowing for truncation of the input space. Second, the remaining inputs are typically highly correlated, further reducing the effective volume of the input space.

To demonstrate the surrogate-based shape optimization procedure, we examine the Stokes drag over an axisymmetric, fore-aft symmetric body. The simulation for which the surrogates are substituted is a finite element solver utilizing an Uzawa nested conjugate gradient iteration. The inputs to the problem are a set of coefficients which describe the shape,  $b(\theta)$ , and the output is the non-dimensional drag,  $F_D$ . The design optimization problem is to find the optimal shape,  $b^*(\theta)$ , for a given target drag,  $\lambda$ :

$$b^*(\theta) = \arg \min_{b(\theta) \in W_+, b(\theta) \leq C(\theta)} |F_D - \lambda|. \quad (19)$$

The general geometry and the physical constraint on the optimal profile,  $C(\theta)$ , are shown in Figure 4.

The surrogate for the Stokes drag over the body is simply the Stokes drag over a sphere of equivalent surface area. Other surrogates such as response surfaces constructed from simulation data could be considered instead. The surrogate-based optimization problem is identical to Equation (19), but the simulation result,  $F_D$ , is replaced by the drag surrogate,  $\hat{F}_D$ .

The quarter-body profile of the shape in the first quadrant describes the full three-dimensional body. The shape is expressed as a positive function  $b(\theta) \in W_+([0, \pi])$ , where  $W_+$  is a set of admissible functions. We introduce a basis for  $W_+([0, \pi])$  and truncate this basis to  $M$  terms. The shape function can then be expressed as

$$b(\theta) = 1 + \sum_{j=1}^M A_j \cos(2j\theta). \quad (20)$$

The result is that the shape profiles are parameterized by  $\mathbf{A}^M = \{A_1, \dots, A_M\}$ , which acts as the input,  $\mathbf{p}$ . The shapes in this problem are described by 10 inputs ( $M = 10$ ).

To generate a random ensemble of shapes for validation, and for Monte Carlo sampling for the proximal-candidate error analysis, a random-shape process inducing an importance function on the set of coefficients is employed (Elishakoff, 1983; Otto, 1995; Otto et al., 1995). With this method, certain smoothness conditions at the endpoints of the shape are enforced, as are

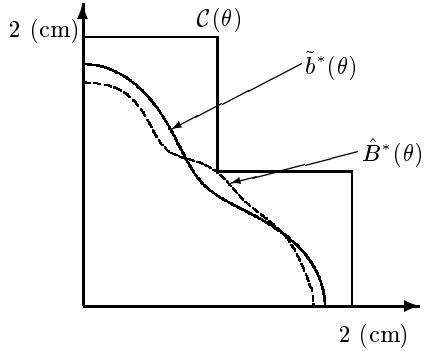


Figure 4: Surrogate predicted optimal and proximal candidate shapes.

statistical quantities of the ensemble, such as the mean and covariance. Through the mean and covariance of the radius-function describing the shape, the designer reflects his prejudices as to the class of shapes that will contain the optimizer.

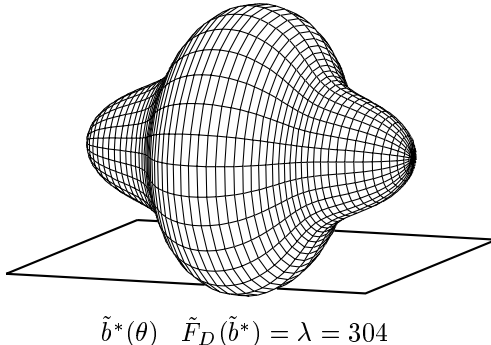
We select  $\eta$ ,  $\varepsilon_2$ , and  $\Delta(\cdot, \cdot)$  and proceed with the validation, the surrogate-based optimization, and the candidate-based *a posteriori* error analysis. For this problem we choose  $\eta = .18$ , and  $\varepsilon_2 = .18$ . The distance criterion chosen,  $\Delta(\cdot, \cdot)$ , is the Hausdorff distance. With Equation (5), and our values of  $\eta$  and  $\varepsilon_2$ , we find that 30 validation points are needed. The resulting model prediction error is  $U = .15$ .

For the design problem, we choose a target drag  $\lambda = 304$  dynes, and find the surrogate-predicted optimizer,  $\tilde{b}^*(\theta)$ . Based on  $\eta = .18$ , we find  $\Delta_{max} = .35$ , using a “best scaled” geometry for the acceptance/rejection. The region in the proximity of the  $\tilde{b}^*(\theta)$  is then queried for a candidate design  $\hat{B}^*(\theta)$ . With this candidate, the following predictability statement can be made: With confidence greater than .82,

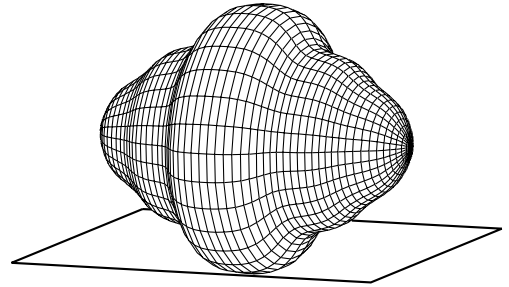
$$\frac{|F_D(\hat{B}) - \lambda|}{\lambda} \leq |1 - \beta^*| + \beta^* U = .18. \quad (21)$$

In words, with confidence greater than .82, the absolute difference between the actual drag on the candidate design and the target drag,  $\lambda = 304$  dynes, normalized by the target drag, will be less than or equal to .18. The coefficient,  $\beta^*$ , present in the final predictability statement results from the scale-invariance (self-similarity) in the linear Stokes drag relation. This coefficient is near one and has the effect of increasing the model prediction error,  $U$ , from .15 to the value .18 present in Equation (21). Three-dimensional plots of the surrogate-predicted optimal design and the proximal-candidate are shown in Figure 5.

A designer can conclude from this result that there is likely to be a design near the surrogate-predicted optimal design which will satisfy the target drag re-



$$\tilde{b}^*(\theta) \quad \tilde{F}_D(\tilde{b}^*) = \lambda = 304$$



$$\hat{B}^*(\theta) \quad F_D(\hat{B}^*) = 312$$

Figure 5: The surrogate-predicted optimal shape (left) and the proximal-candidate design (right). The target drag,  $\lambda$ , and, the simulation-predicted Stokes drag of the proximal-candidate are indicated.

quirement to within 18%. If this is deemed satisfactory, the designer can consider the process a success. The advantage of this approach is that, at this point, the designer can explore other objective functions using the same validated surrogate, without the need for additional simulation evaluations.

If the error reflected on the right side of Equation (21) is deemed too large, it can be reduced by an improved surrogate, which could be accomplished, say, by dedicating a portion of the simulation evaluations to the construction of a response surface. A response surface would likely introduce a finite  $\delta'$  in (10) (not present for the simple surrogate presented here). To reduce  $\delta'$ , a smaller prediction region  $\mathcal{R}$  (physically) is necessary, which requires a smaller  $\varepsilon_1$  and, therefore, either more validation points or a better  $\rho(\mathbf{p})$  (one that more accurately anticipates the “location” of the optimizer).

## ACKNOWLEDGMENTS

This work was supported by the ARPA under Grant N00014-91-J-1889, by the ONR under Grants N00014-90-J-4124 and N00014-89-J-1610, by the AFOSR under Grant F49620-94-1-0121, and by NASA under Grant NAG 1-1613. We would also like to acknowledge an FCAR Aeronautical Scholarship (M.P.) and the NASA Graduate Training Program (J.O.).

## REFERENCES

- Barthelemy, J.-F. M., and Haftka, R.T., 1993, “Approximation Concepts For Optimum Structural Design — A Review,” *Structural Optimization*, **5**, pp. 129–144.
- Bohlin, T., 1991, *Interactive System Identification: Prospects and Pitfalls*, Springer-Verlag, Berlin.
- David, H. A., 1981, *Order Statistics*, 2nd ed., John Wiley and Sons, New York.
- Elishakoff, I., 1983, *Probabilistic Methods in the Theory of Structures*, John Wiley and Sons, New York.
- McKay, M. D., Beckman, R. J., and Conover, W. J., 1979, “A Comparison of Three Methods For Selecting

Values of Input Variables In the Analysis of Output from a Computer Code,” *Technometrics*, **21**, pp. 239–245.

Newman, P. A., Hou, G. J.-W., Jones, H. E., Taylor III, A. C., and Korivi, V. M., 1992, “Observations on Computational Methodologies For Use in Large-Scale, Gradient-Based, Multidisciplinary Design,” AIAA Paper 92-4753.

Otto, J. C., 1995, Ph.D. Thesis, Massachusetts Institute of Technology, Cambridge, MA, in progress.

Otto, J. C., Paraschivoiu, M., Yeşilyurt, S., Patera, A. T., 1995 “Bayesian-Validated Computer-Simulation Surrogates For Optimization and Design,” *Proceedings, ICASE Workshop on Multidisciplinary Design Optimization*, Hampton, VA, SIAM.

Paraschivoiu, M., 1995, Ph.D. Thesis, Massachusetts Institute of Technology, Cambridge, MA, in progress.

Sacks, J., Welch, W. J., Mitchell, T. J., and Wynn, H. P., 1989 “Design and Analysis of Computer Experiments,” *Statistical Science*, **4**, pp. 409–435.

Seber, G. A. F., and Wild, C. J., 1989, *Nonlinear Regression*, John Wiley & Sons, New York.

Shepard, D., 1968, “A Two-Dimensional Interpolation Function For Irregularly Spaced Data,” *Proc. 23rd Nat. Conf.*, pages 517–524, ACM.

Valiant, L. G., 1984, “A Theory For the Learnable,” *CACM*, **27**, pp. 1134–1142.

Yeşilyurt, S., 1995, “Construction and Validation of Computer-Simulation Surrogates For Engineering Design and Optimization,” Ph.D. Thesis, Massachusetts Institute of Technology, Cambridge, MA.

Yeşilyurt, S., Ghaddar, C., Cruz, M., and Patera, A. T., 1995, “Bayesian-Validated Surrogates For Noisy Computer Simulations; Application To Random Media,” *SIAM J. Sci. Comput.*, to appear.

Yeşilyurt, S., and Patera, A. T., 1995, “Surrogates For Numerical Simulations; Optimization of Eddy-Promoter Heat Exchangers,” *Comp. Methods Appl. Mech. Engr.*, **121**, pp. 231–257.

# **COMPUTER-SIMULATION SURROGATES FOR OPTIMIZATION: APPLICATION TO TRAPEZOIDAL DUCTS AND AXISYMMETRIC BODIES**

by

**John C. Otto**

Department of Aeronautics and Astronautics, M.I.T.  
Multidisciplinary Design Optimization Branch  
NASA Langley Research Center  
Hampton, Virginia

**Marius Paraschivoiu, Serhat Yeşilyurt, and Anthony T. Patera**

Department of Mechanical Engineering  
Massachusetts Institute of Technology  
Cambridge, Massachusetts

July 10, 1995

In the Proceedings of the Forum on CFD for Design and Optimization, ASME International Mechanical Engineering Conference and Exposition, November 12–17, 1995, San Francisco, CA. Address all correspondence to: John C. Otto, Mail Stop 159, NASA Langley Research Center, Hampton, VA 23681-0001, U.S.A.